AIP | Applied Physics Letters

Precise control of epitaxy of graphene by microfabricating SiC substrate

H. Fukidome, Y. Kawai, F. Fromm, M. Kotsugi, H. Handa et al.

Citation: Appl. Phys. Lett. **101**, 041605 (2012); doi: 10.1063/1.4740271
View online: http://dx.doi.org/10.1063/1.4740271
View Table of Contents: http://apl.aip.org/resource/1/APPLAB/v101/i4
Published by the American Institute of Physics.

Precise control of epitaxy of graphene by microfabricating SiC substrate

H. Fukidome,[1,a)] Y. Kawai,[2] F. Fromm,[3] M. Kotsugi,[4] H. Handa,[1] T. Ide,[1] T. Ohkouchi,[4] H. Miyashita,[2] Y. Enta,[5] T. Kinoshita,[4] Th. Seyller,[3] and M. Suemitsu[1]
[1]*Research Institute of Electrical Communications, Tohoku University, 2-1-1 Katahira, Aoba-ku, Sendai 980-8577, Japan*
[2]*School of Engineering, Tohoku University, 6-6-01 Aramaki, Sendai 980-8579, Japan*
[3]*Lehrstuhl für Technische Physik, Universität Erlange-Nürnberg, Erwin-Rommel-Str.1, 91058 Erlangen, Germany*
[4]*JASRI/SPring-8, 1-1-1 Kouto, Sayo-cho, Sayo-gun, Hyogo 679-5148, Japan*
[5]*Graduate School of Science and Technology, Hirosaki University, Aomori 036-8561, Japan*

(Received 30 April 2012; accepted 17 July 2012; published online 27 July 2012)

Epitaxial graphene (EG) on SiC is promising owing to a capability to produce high-quality film on a wafer scale. One of the remaining issues is microscopic thickness variation of EG near surface steps, which induces variations in its electronic properties and device characteristics. We demonstrate here that the variations of layer thickness and electronic properties are minimized by using microfabricated SiC substrates which spatially confines the epitaxy. This technique will contribute to the realization of highly reliable graphene devices. © *2012 American Institute of Physics*. [http://dx.doi.org/10.1063/1.4740271]

Graphene is becoming a promising material in a variety of fields, such as electronics,[1–3] photonics,[4] and even spintronics,[5] due to its unique physical properties, e.g., tunable bandstructures.[6–8] For device applications, one of the key issues is to prepare high-quality graphene films on a wafer scale. Epitaxial graphene (EG) obtained by thermal decomposition of SiC is a viable route for wafer-scale synthesis of high quality graphene films.[9] The capability of EG has been in fact demonstrated recently as the active material for integrated circuits.[3]

One of the remaining issues of EG is to suppress the microscopic thickness variation due to unintentional nucleation of graphene near SiC surface steps.[9] The electronic structure and device characteristics of graphene are susceptible to layer thickness.[6,8–10] For highly reliable graphene devices, reduction of the step density on SiC surfaces is therefore a prerequisite.

One possible solution for the reduction of the step density is to spatially confine the surface reactions by using substrate microfabrication.[11,12] It has been demonstrated that spatial confinement of surface reactions on Si surfaces, e.g., homoepitaxy and sublimation, on microfabricated Si substrates induces self-ordering of steps and even step-free surfaces.[11,12] On EG formation on SiC, the Si sublimation from the SiC surface is the key reaction,[9] so that effective spatial confinement of Si sublimation is anticipated to suppress the step density and the microscopic thickness variation. Studies on epitaxial graphene on structured SiC substrates have already been made, but to form graphene nanoribbons at edges of the microstructures.[13,14] No EG was formed in the center of the microstructures. No clear relationships among the substrate microfabrication, the step density, and the thickness variation of EG have been established yet.

In this letter, we clearly demonstrate that epitaxy of graphene on microfabricated SiC(0001) makes it possible to suppress the thickness variation. This epitaxy is effective also for controlling structural and even electronic properties of EG.

As a reference to the epitaxy of graphene on microfabricated SiC(0001), structural and electronic properties of EG on a non-fabricated SiC(0001) were investigated, as shown in Fig. 1. EG was formed by annealing the SiC(0001) (n-type, 0.01 Ω cm) at 1923 K in Ar ambience[9] using a custom build oven.[15] Figure 1(a) shows an image of EG taken by low-energy electron microscopy (LEEM). The brighter and the darker regions, and the finger-like features are imaged,[16] as indicated by white arrows in the LEEM image. Figure 1(b) shows the electron reflectivity spectra of them, taken from the LEEM images.[17] In the spectra, the dips result from the resonant electron transmission through quantized conduction band states of graphene, whose wave vectors are normal to the graphene films.[17] A single dip exists in the spectrum from the brighter regions and the finger-like features as well, while two dips exist in the spectrum from the darker region. Since the number of dips corresponds to graphene layer thickness,[17] the brighter and the darker regions are identified as monolayer and bilayer graphene, respectively. In the same manner, the finger-like features are identified also as monolayer graphene. The finger-like features are, however, believed to possess a slightly different electronic structure from that of ordinary monolayer graphene (the brighter region). The electron reflectivity spectrum of the finger-like feature shows a blueshift in its dip position. This blueshift suggests that the finger-like feature has a smaller work function than the monolayer graphene regions since the dip position of the monolayer graphene corresponds to the conduction band level at the A point ($E_{dip} = E_F + 7.0\,eV$) along the Γ-A direction normal to the graphene sheet.[17] To verify this, the very same surface of EG was imaged by photoelectron emission microscopy with a Hg lamp (cutoff

a)Author to whom correspondence should be addressed. Electronic mail: fukidome@riec.tohoku.ac.jp.

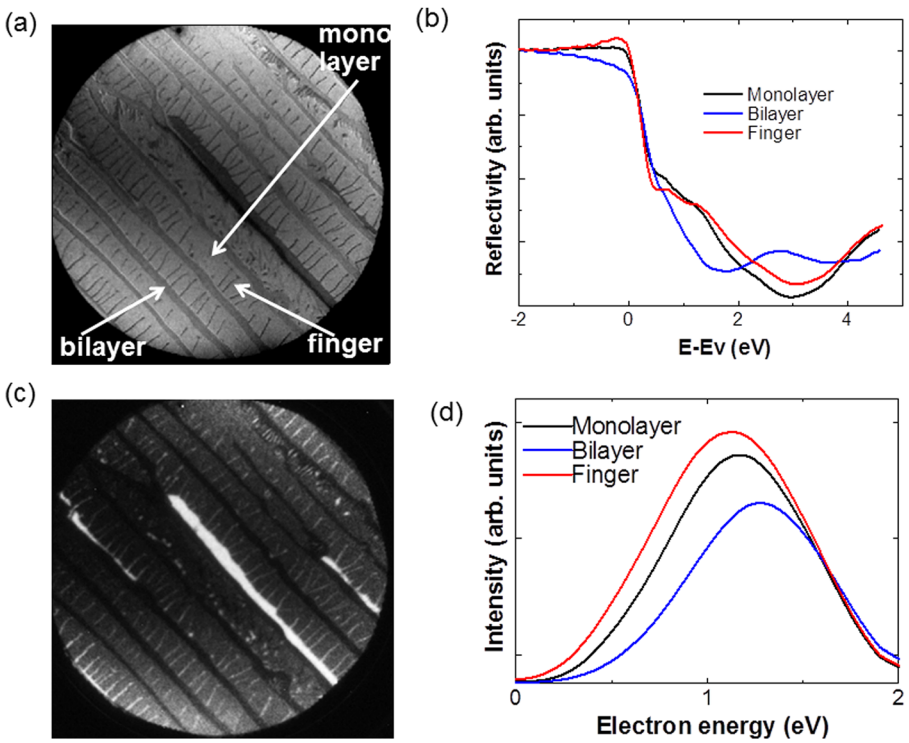

FIG. 1. (a) LEEM image of EG (field of view: 35 μm). The incident electron energy is 0.5 eV. (b) The electron reflectivity spectra of monolayer, bilayer, and finger-like features, which are indicated by white arrows. (c) UV-PEEM image of EG (Field of view: 35 μm). The kinetic energy of collected electrons for the imaging is 1 eV. (d) The onsets of photosecondaries of monolayer, bilayer, and finger-like features.

energy: ~5 eV) as a light source (UV-PEEM), as shown in Fig. 1(c). The contrast in this UV-PEEM image reflects the difference in the yield of electron emission at photothreshold, which is in many cases related to work function.[18] Figure 1(d) shows the onsets of photosecondaries of monolayer, bilayer, and finger-like features. It is revealed that the work function of bilayer graphene is larger than that of monolayer graphene. This result is consistent with a previous report.[19] In addition, the work function of the finger-like feature is determined to be smaller than that of monolayer graphene, consistent with the electron reflectivity spectra (Fig. 1(b)). The structure (layer thickness) and the electronic properties (work function) of EG thus fluctuate when formed without substrate microfabrication.

The fluctuations of EG are suppressed drastically on microfabricated SiC(0001) substrates. The microfabrication was done by using conventional electron beam lithography and fast atomic beam etching.[20] Figure 2(a) shows a typical LEEM image of the epitaxial graphene on the microfabricated SiC(0001) (μ-EG). The microscopic thickness variation almost disappears in smaller patterns, e.g., pattern A (side length: 5 μm), while the variation exists in larger patterns like B (side length: 6 μm) and C (side length: 7 μm). Figure 2(b) shows a C1s core-level PEEM image. At the kinetic energy (61.25 eV) for the imaging, the C1s peak of graphene is dominant. In larger patterns of B and C, thicker graphene layers (brighter regions) indicated by the white arrows are visible, in addition to monolayer regions (the darker region). On the other hand, only the monolayer region (the darker region) is visible in pattern A. This accords with the LEEM contrast (Fig. 2(a)). The suppression of the thickness variation in smaller patterns is realized by decreasing the density of surface step which induces unintentional formation of multilayer graphene. The surface step density decreases on the smaller patterns by gathering the surface steps at the peripheries of the patterns.[11] The threshold size of the triangle pattern is about 5 μm. Details of the suppression shall be explained later, by using Fig. 4.

The substrate microfabrication is influential to compressive strain due to a difference in a thermal expansion between graphene and SiC. Figure 2(c) compares the Raman spectra for four different sizes of μ-EG pattern. In all the spectra, sharp G and G′ bands of graphene are detected, while D bands (~1360 cm^{-1}) originating from the presence of the defects in graphene are not detected. This indicates that μ-EG in the patterns does not contain an appreciable amount of defects.[21] Figure 2(d) shows the compressive strain estimated from the peak position of the G′ band,[22] as a function of the pattern size. The compressive strain becomes stronger by reducing the pattern size. This increased compressive strain can be related to the reduction of the defect density in smaller patterns. A similar negative correlation between the defect density and the compressive strain can be found between a low-quality EG produced in ultrahigh-vacuum annealing and a high-quality EG produced in Ar ambience.[10]

The impact of the microfabrication on carrier doping is inferred also from the Raman spectra. Figure 2(e) shows the peak shift of the G band due to electron doping in graphene. The peak shift due to the compressive strain (ΔG_{strain}) is subtracted by using the G′ band peak position with the relation $\Delta G'_{strain}/\Delta G_{strain} = 2.1$.[22] We find that the peak shift of the G band due to electron doping is smaller in μ-EG on smaller patterns. We therefore suggest that the work function of μ-EG becomes larger by reducing the pattern size. This can be corroborated by measuring the electron reflectivity spectra of μ-EG. Figure 3(a) shows typical electron reflectivity spectra of μ-EG. Figure 3(b) shows the dependence of the dip position on the pattern size. It is clarified that the dip position redshifts by reducing the pattern size. This redshift can be

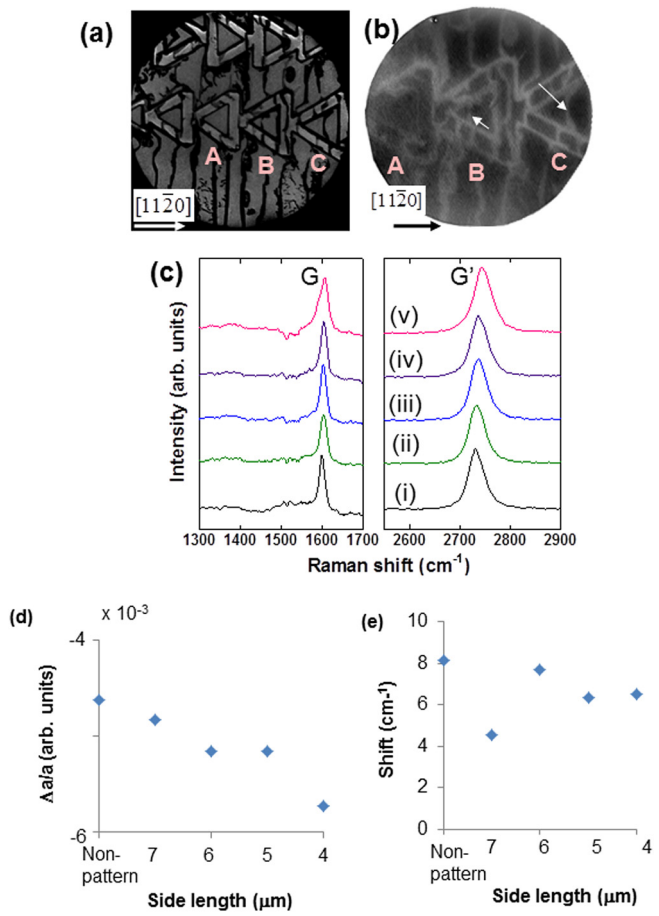

FIG. 2. (a) LEEM image of μ-EG (Field of view: 50 μm). The incident electron energy is 2.2 eV. (b) C1s core level PEEM image of μ-EG (Field of view: 35 μm). The incident photon energy is 350 eV. The kinetic energy of photoemitted electron is 61.25 eV with the energy resolution of 0.5 eV. The white arrows indicate the thicker graphene regions in pattern B and C. (c) Raman spectra of an epitaxial graphene on non-patterned region (i) and μ-EG whose lengths of a side are 7 μm (ii), 6 μm (iii), 5 μm (iv), and 4 μm (v). (d) The lattice constant change due to compressive strain. (e) The estimated shift of the G band due to electron doping.

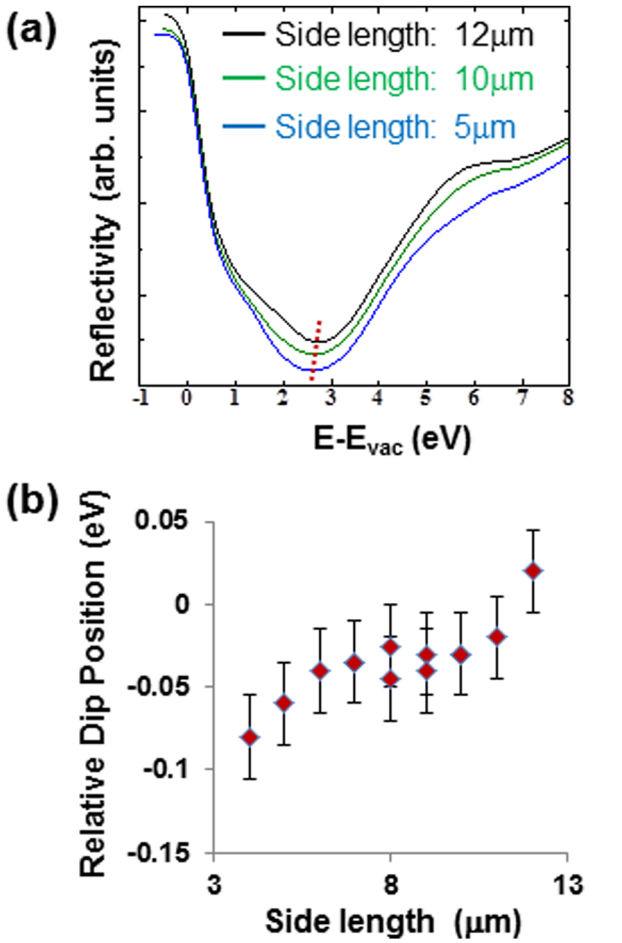

FIG. 3. (a) Typical electron reflectivity spectra of μ-EG on different pattern sizes. (b) Dip positions of the electron reflectivity spectra of μ-EG on different pattern sizes, relative to that of EG on the non-patterned region.

explained by the increase in the work function of graphene, as discussed above (Figs. 1(b) and 1(d)). It is therefore concluded that the epitaxy on smaller patterns can produce higher quality μ-EG with less electron doping and larger compressive strain. The increase in work function may be ascribed to the reduction of defect density which contributes unintentional electron doping in graphene and also relieves the compressive strain.

The variation of graphene thickness is believed to originate from the step recession and collection of steps at the periphery of the pattern during graphitization. To verify the relation between the nucleation of graphene and the step, the effects of the pattern shape and size on the thickness variation of μ-EG are investigated by LEEM and atomic force microscopy (AFM). Figures 4(a) and 4(b) show LEEM and AFM images of μ-EG in the rectangle patterns whose dimensions are varied in the direction of [11$\bar{2}$0], respectively. For μ-EG on larger rectangular patterns (A1, B1, and C1), a comparison of the LEEM image with the AFM image indicates that bilayer graphene exists near steps, probably due to random nucleation near the steps. On the narrow patterns with side lengths below 1 μm (D1, E1, and F1), the LEEM image shows that bilayer as well as the finger-like features diminishes in μ-EG. Furthermore, the surfaces of the narrow patterns are step-free, as shown in the AFM image. On the other hand, both thickness variation and surface step density do not change by shortening the length of the side in the [1100] direction, as shown by LEEM (Fig. 4(c)) and AFM (Fig. 4(d)). The reduction of the side length in the [11$\bar{2}$0] direction is thus proven to be effective for the reduction of the thickness variation. The threshold size of the rectangular pattern is about 1 μm, which means that the uniform monolayer graphene is formed on the small pattern whose side length in the [11$\bar{2}$0] direction is less than 1 μm.

This result can be explained as follows. The suppression of the thickness variation is achieved by decreasing the surface step density, which nucleates uncontrolled number of graphene layers.[9] The decrease of surface step density on smaller patterns is understood in analogy with the reduction of surface step density on microfabricated Si substrate.[11] On the smaller patterns, the surface diffusion length of surface adspecies emitted during the step retreat becomes larger than the length of the patterns in the direction of the step retreat. The surface steps are then gathered at the edges of patterns. The difference in threshold size of triangular and rectangular patterns may be attributed to the change in mutual angles between the step retreat direction and the direction of the side of the pattern.

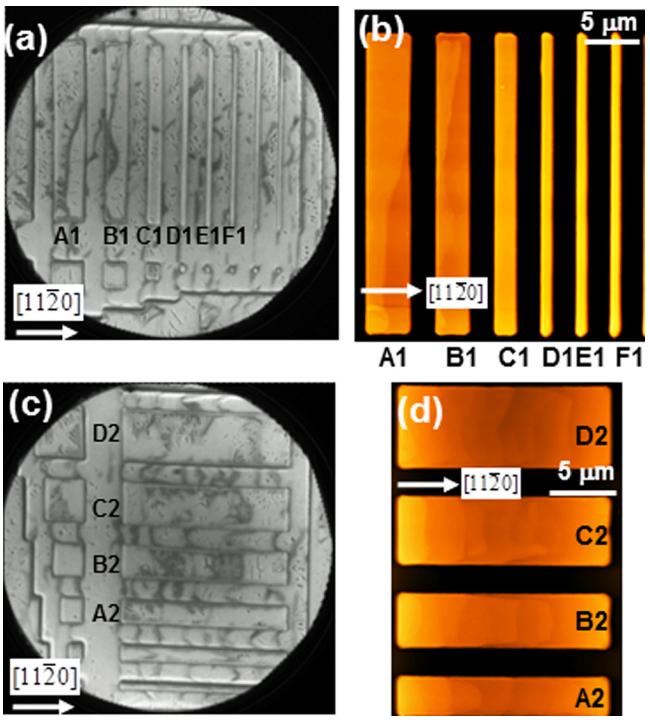

FIG. 4. (a, b) LEEM and AFM images of μ-EG on the patterns whose side lengths vary in the direction of [11$\bar{2}$0], respectively. (c, d) LEEM and AFM images of μ-EG on patterns whose side lengths vary along [1100], respectively. Field of view of the LEEM images (a, c) is 50 μm.

In conclusion, we have succeeded in producing high-quality epitaxial graphene without thickness variation by spatially confining the epitaxy of graphene using a microfabrication patterning of the SiC(0001) substrate. Furthermore, the spatial confinement makes it possible to control the structural and electronic properties of the epitaxial graphene. This novel technique will boost the development of electronic devices based on epitaxial graphene.

We gratefully acknowledge Professor K. Horn for critical reading for the manuscript and insightful discussions. Part of this work is supported by MEXT as Specially Supported Research (23000008) and Scientific Research (C) (23560003). Work in Erlangen was supported by the German Research Council (DFG) and by the European Science Foundation (ESF) through SE 1087/7-1 and SE 1087/9-1. Part of this work was performed at BL17SU of SPring-8 as Nano-technology Support Project of MEXT (2009B1735, 2010A1674, and 2010B1712). Microfabrication of SiC(0001) substrates was done at Micro/Nano-Machining Research and Education Center, Tohoku University.

[1]K. V. Novoselov, A. K. Geim, S. V. Morozov, D. Jiang, Y. Zhang, S. V. Dubonos, I. V. Grigorieva, and A. A. Firsov, Science **306**, 666 (2004).
[2]C. Berger, Z. Song, T. Li, X. Li, A. Y. Ogbazghi, R. Feng, Z. Dai, A. N. Marchenkov, E. H. Conrad, P. N. First, and W. A. de Heer, J. Phys. Chem. B **108**, 19912 (2004).
[3]Y.-M. Lin, A. Valdes-Garcia, S.-J. Han, D. B. Farmer, I. Meric, Y. Sun, Y. Wu, C. Dimitrakopoulos, A. Grill, Ph. Avouris, and K. A. Jenkins, Science **332**, 1294 (2011).
[4]F. Bonaccorso, Z. Sun, T. Hasan, and A. C. Ferrari, Nature Photon. **4**, 611 (2011).
[5]H. Goto, A. Kanda, T. Sato, S. Tanaka, Y. Ootuka, S. Okada, H. Miyazaki, K. Tsukagoshi, and Y. Aoyagi, Appl. Phys. Lett. **92**, 212110 (2008).
[6]A. H. Castro Neto, F. Guinea, N. M. R. Peres, K. V. Novoselov, and A. K. Geim, Rev. Mod. Phys. **81**, 109 (2009).
[7]M. Sprinkle, D. Siegel, Y. Hu, A. Tejeda, A. Taleb-Ibrahimi, P. Le Fèvre, F. Bertran, S. Vizzini, H. Enriquez, S. Chiang, P. Soukiassian, C. Berger, W. A. de Heer, A. Lanzara, and E. H. Conrad, Phys. Rev. Lett. **103**, 226803 (2009).
[8]T. Ohta, A. Bostwick, Th. Seyller, K. Horn, and E. Rotenberg, Science **313**, 951 (2006).
[9]K. V. Emstev, A. Bostwick, K. Horn, K. Jobst, G. L. Kellogg, L. Ley, J. L. McChesney, T. Ohta, S. A. Reshanov, J. Röhrl, E. Rotenberg, A. K. Schmid, D. Waldmann, H. B. Weber, and Th. Seyller, Nature Mater. **8**, 203 (2009).
[10]W. Zhu, V. Perebeinos, M. Freitag, and P. Avouris, Phys. Rev. B **80**, 235402 (2009).
[11]Y. Homma, N. Aizawa, and T. Ogino, Jpn. J. Appl. Phys. Part 2 **35**, L241 (1996).
[12]S. Tanaka, C. C. Umbach, J. M. Blakely, R. Tromp, and M. Mankos, Appl. Phys. Lett. **69**, 1235 (1996).
[13]M. Sprinkle, M. Ruan, Y. Hu, J. Hankinson, M. Rubio-Roy, B. Zhang, X. Wu, C. Berger, and W. A. de Heer, Nat. Nanotechnol. **5**, 727 (2010).
[14]W. A. de Heer, C. Berger, M. Ruan, M. Sprinkle, X. Li, Y. Hu, B. Zhang, J. Hankinson, and E. Conrad, Proc. Natl. Acad. Sci. U.S.A. **108**, 16900 (2011).
[15]M. Ostler, F. Speck, M. Gick, and Th. Seyller, Phys. Status Solidi B **247**, 2924 (2011).
[16]T. Ohta, N. C. Bartelt, S. Nie, K. Thürmer, and G. L. Kellog, Phys. Rev. B **81**, 121411 (2010).
[17]H. Hibino, H. Kageshima, F. Maeda, M. Nagase, Y. Kobayashi, and H. Yamaguchi, Phys. Rev. B **77**, 075413 (2008).
[18]C. M. Schneider and G. Schönhense, Rep. Prog. Phys. **65**, R1785 (2002).
[19]H. Hibino, H. Kageshima, M. Kotsugi, F. Maeda, F.-Z. Guo, and Y. Watanabe, Phys. Rev. B **79**, 125437 (2009).
[20]T. Ide, Y. Kawai, H. Handa, H. Fukidome, M. Kotsugi, T. Ohkochi, Y. Enta, T. Kinoshita, and M. Suemitsu, Jpn. J. Appl. Phys. **51**, 06DF02 (2012).
[21]F. Tuinstra and J. L. Koenig, J. Chem. Phys. **53**, 1126 (1970).
[22]F. Speck, J. Jobst, F. Fromm, M. Ostler, D. Waldmann, M. Hundhausen, H. B. Weber, and Th. Seyller, Appl. Phys. Lett. **99**, 122106 (2011).